CrossMark

ORIGINAL ARTICLE

Non-destructive and on site method to assess the air-permeability in dimension stones and its relationship with other transport-related properties

**B. Sena da Fonseca · A. S. Castela ·
R. G. Duarte · R. Neves · M. F. Montemor**

Abstract This work studies the suitability of the "Torrent" air-permeability test method for testing dimension stones. To test its feasibility, measurements were performed on stone slabs with porosities in the range of 0.2–17.2 %. Statistically, accurate and reliable measurements were achieved on stones with open porosities above 2 %. Close relations were found between air-permeability coefficient and other transport-related properties. Therefore, the air-permeability coefficient can be a parameter, on its own, providing useful information about the stone susceptibility to decay. Moreover, a graded classification is suggested with the purpose of providing information for a proper application of stones in constructions.

Keywords Dimension stone · Air-permeability · Torrent · Porosity · Water absorption · Decay

1 Introduction

Dimension stones have been widely employed on modern buildings and are also present in historic

B. Sena da Fonseca (✉) · A. S. Castela ·
R. G. Duarte · M. F. Montemor
ICEMS-DEQ, Instituto Superior Técnico, ULisboa,
1049-001 Lisbon, Portugal
e-mail: senadafonseca@gmail.com

A. S. Castela · R. G. Duarte · R. Neves
Instituto Politécnico de Setúbal, ESTBarreiro,
2839-001 Barreiro, Portugal

heritage, including monuments and sculptures [3, 25, 61]. When in service, the dimension stones are exposed to the action of physical and chemical weathering. Water is the most important abiotic factor of stone degradation and is the main vehicle carrying harmful agents [30, 45, 51]. Water capture occurs according to its exposure to rain, groundwater, condensation and humid air to be released by the drying conditions of atmosphere [18]. It penetrates into any open capillary channels and the degree of moisture inside the stone depends on their hydraulic properties, which in turn, influences the material durability [1, 2, 14, 33, 51]. At the forefront of such influencing properties are the porosity and pore characteristics such as pore size, morphology, tortuosity, connectivity and size variation. Low porous stones are generally found to be more durable since water will be less able to penetrate and thus, less able to promote damage [22]. Closely linked to all of these physical features is the permeability of the stone [38, 42]. The main decay processes related to open porosity and hydraulic properties, including permeability, that could be appointed are salts and ice crystallization and chemical dissolution [27, 30, 31]. The salts and ice crystallization are in general more severe in stones with higher porosity and permeability once water penetrates easily and faster. In internal zones, the stresses caused by crystal growth on pore walls are more damaging in internal zones where the space is more confined while in surface the crystals can growth outwards. In particular cases of high porous stones (>30 %), the structure is so open

rilem

that the available pore space can accommodate any expansion generated during freezing or salt growth [22].

Similarly, high hydraulic connectivity allows further penetration of acidic water from polluted atmospheres or other non neutral solutions (e.g. cleaning products).

Depending on the lithotype, several others phenomena and degradation mechanisms could emerge. Regarding sedimentary stones, namely the carbonates with similar chemical composition and stability, the cementing processes manage the compactness. In these stones, the compactness and porosity are two connected concepts [53] and the stone matrix has also an important role in the mechanical performance. Since the action of salt and ice crystallization is essentially mechanical, the matrix consolidation has also an important influence on stone susceptibility to decay. Without disregarding this aspect, once the porosity gives an indirect idea about the matrix compaction degree, the knowledge of stone behavior subjected to moisture is essential in any application as dimension stone and provides fundamental indications about its weathering resistance. There are several standardized tests used to predict the stone response against water as a decay agent: determination of open porosity [8], water absorption by capillarity [7], water absorption at atmospheric pressure [9], water penetration by RILEM tube [12], drying behavior [11] or water vapor permeability [10].

Furthermore, these tests are used in the study of stones alteration owing to weathering processes [2, 54] and in the evaluation of the performance of surface treatments [16, 40, 43, 44, 47]. With the exception of water penetration by RILEM tube [21] all the other tests are performed in laboratorial conditions and the samples must comply with geometric requirements. Moreover, such tests have a destructive nature. Samples of dimension stones in service are usually obtained by core drilling or other destructive methods. In this field, efforts have been made to develop alternative and non-destructive analysis methods [29].

As mentioned, the permeability of materials, as stones, is defined by the properties that characterize the penetration of water and gases and it depends mainly on the characteristics of porous media [26]. Several methods are available to measure in situ the air-permeability of concrete surface, namely, the method developed by R. Torrent described as "Torrent

Permeability Test Method". This method is gaining acceptance, evidenced by the considerable amount of publications in which it has been referred and by its recent inclusion in the Swiss standard SIA 262/1-E [50], updated in 2013. It has been used as a very useful method to measure the air-permeability and to give helpful indications about concrete durability [6].

According to the equipment brochure [32] this non-destructive site permeability test is also applicable to other materials such as stones. However, in dimension stones, similar approaches are quite unusual and literature about its application on rock is scarce [4].

In concrete, the comparative data between this air-permeability coefficient and other transport properties revealed some interesting relationships [36, 56].

Considering the state-of-art, the present work aims at assessing the viability and accuracy of Torrent permeability test method to assess the air-permeability coefficient of dimension stones. The results were compared with other physical transport-related properties: grain size, open porosity, water absorption, capillary suction coefficient and evaporation parameters, in order to evaluate relationships. Interesting agreement was found between these properties and air-permeability values highlighting their close interdependency.

These characteristics are commonly used as indicators of stone durability and therefore the air-permeability coefficient may also provide useful indications on stone susceptibility to decay.

2 Materials and methods

2.1 Stones general features

Fifteen varieties of stones quarried in different regions of Portugal were used in this investigation. Chemically, the stones are limestones and marbles, both mainly composed by $CaCO_3$. The stones have different textural relations inherent to their facies and different degrees of crystallization. As these aspects affect the pore-network characteristics, the selection of the stones was made to obtain a wide range of different transport-related features.

The commercial trade name of the stones was adopted in present work for simplification. The studied stones varieties and the respective quarrying locations are exhibit in Table 1.

Table 1 Used stone varieties and its quarrying locations

Commercial trade name	Reference	Quarrying location
Ataíja Azul	AA	Ataíja, District of Santarém
Azul Valverde	AV	Covão Alto, District of Santarém
Creme Cascais	CC	Porto de Mós, District of Leiria
Estremoz Creme	EC	Vila Viçosa
Fátima Creme	FC	Fátima, District of Ourém
Gascaigne Beige	GB	Alcobaça, District of Leiria
Gascaigne Blue	GBl	
Lioz	L	Pêro Pinheiro, District of Lisboa
Moca Creme Fino	MCf	Alcanede, District of Santarém
Moca Creme Grosso	MCg	
Moleanos "Classic"	MC	Alcobaça, District of Leiria
Moleanos M8	M8	
Moleanos Rijo	MR	
Rosal AR or *Salgueira*	RA	Arrimal, Porto de Mós
Rosal Fleuri	RF	Serro Ventoso, Porto de Mós

All the lithotypes are commercialized in slabs of various dimensions and in elements with other geometrical shapes are sold by the manufacturing companies as a building material for multiple purposes. Several surface finishes are possible; polished, honed, bush-hammered, brushed or flamed. The main applications are external cladding in facades, masonry, internal flooring, external pavements and internal walls, all over the world.

2.2 Torrent permeability test method

The "Torrent Permeability Tester Method" was developed at *Holcim Group Support Ltd.* in Switzerland [55]. The method is applicable to concrete, rock, stone, clay products, ceramics, etc. [32].

In this work, the commercial equipment "Permea-Torr" was used. The permeability measurements with this apparatus are non-destructive. Measurements can be taken on site as well as in laboratory conditions, which are major advantages when compared to other permeability-testing apparatus. Additionally, the equipment allows fast and fully automatic measurements [32].

The test with this device starts with the creation of a vacuum inside the two chamber cell, which is sealed on the material surface by means of concentric rubber rings, creating two separate chambers. When vacuum reaches 30 mbar, the valve of inner chamber is closed. The air in the pores flows through the material into the inner chamber, raising its pressure. The rate of pressure rise with time is directly linked to the coefficient of air-permeability of the material surface [57].

A pressure regulator maintains the pressure of external chamber permanently balanced with that of the inner chamber. Therefore, a controlled unidirectional flow into the inner chamber is ensured and the coefficient of air-permeability (kT) is determined according to the equation [32]:

$$kT = \left(\frac{V_c}{A}\right)^2 \frac{\mu}{2\varepsilon P_a} \left(\frac{\ln\frac{P_a + \Delta P_i(t_f)}{P_a - \Delta P_f(t_f)}}{\sqrt{t_f} - \sqrt{t_0}}\right)^2 \tag{1}$$

where kT is the coefficient of air-permeability (m^2), V_c is the volume of inner cell (m^3), A is the cross sectional area of inner cell (m^2), μ is the viscosity of the air, ε is the estimated porosity, P_a is the atmospheric pressure (N/m^2), ΔP_i is the pressure rise in the inner chamber at the end of the test (N/m^2), t_f is the time at the end of the test (s) and t_0 is the time at the beginning of the test (60 s).

The intrinsic factors of the materials that influence the air-permeability value are: total volume of pores, relation of pores size, pore geometry, complexity of the connections between pores (tortuosity) and presence/nature of micro-cracks.

Several researchers have shown that in concrete, kT correlates well with other durability-related properties, namely the water absorption at atmospheric

pressure, water absorption under pressure, carbonation, Cl⁻ penetration [13] and O_2 permeability [57].

2.3 Test methodology

The lithotypes textural analysis was made by macroscopic inspection and through binocular stereoscope observations (Nikon SMZ1000).

A Permea-TORR® equipment was used for air-permeability tests by Torrent method on slabs of $150 \times 150 \times 20$ mm³. After drying at least 3 weeks at room temperature, to ensure removal of remaining moisture the stone samples were oven-dried at 70 °C for 48 h followed by 1 week at room temperature (around 20 °C and R.H. of 60). At this stage all samples were in equilibrium with surrounding environment and considered fairly dry. The moist condition of samples could be very important on the determination of kT values; on moist concrete the absolute values of kT are underestimated. Some deep investigations to improve the method in concrete with a certain degree of water can be found in previous works [13, 46]. In this research the influence of water on kT measurements is not expected, since all the stones were fairly dry when the tests were performed.

Two slabs of each stone variety were used and four measurements were made on polished surfaces and other four on honed surfaces (total of eight measurements per stone variety). The measurements, at the same point, were performed with a gap of 48 h to guarantee that the vacuum created by previous measurement was already dissipated at the beginning of each new measurement.

The open porosity (P_o) and apparent density (ρ_b) values of each stone were assessed according to EN 1936 standard [8]. For saturation, three samples of $50 \times 50 \times 20$ mm from each lithotype were placed in a container under vacuum for 24 h, and then the container was filled with distilled water and the samples remained immersed and under vacuum for another 24 h. After this period, the pressure was increased until atmospheric pressure and the samples stayed under water for another 24 h.

The water absorption at atmospheric pressure (A_b) was determined on three stone samples per variety of $50 \times 50 \times 20$ mm and followed the procedure described in EN 13755 [9]. The vessel with the sample therein was partially filled with distilled water up to half the height of the samples. After 1 h, more water was added until 3/4 of the height. After 2 h, the samples were completely immersed and kept under these conditions until constant mass was achieved.

The water absorption by capillary (AC) was performed according to standard EN 15801 [10]. Three stone samples of each variety ($50 \times 50 \times 20$ mm) were placed in a closed container on a pile of filter papers, approximately 10 mm thickness, partially immersed in water. This setup allows the stone to absorb water upward by capillary forces.

According to Vandevoorde et al. [60], the results provided by this method do not reveal significant differences when compared with others, where the surface of the stone is laid in direct contact with water.

At the end of the capillary test, the lateral faces of the samples were sealed with water impermeable aluminum foil and immersed in distilled water at atmospheric pressure until constant mass. Afterwards, the evaporation test was made in a chamber at 20 °C and 65 % R.H., with potential evaporation of 0.058 mm/h (experimentally calculated). The gravimetric measurements were carried out every hour during the first 8 h and then twice a day, as recommended in EN 16322 (CEN [11] Conservation of cultural property: Determination of drying properties. EN 16322. Commission 25-PEM R [12]). Usually, the first drying phase rate (D_I) and the second drying phase rate (D_{II}) can be calculated from the drying curves. However the calculation of the drying index may be more appropriate for materials which do not exhibit a clear drying curve according with the mechanism of first and second drying phase, as it is the case. The drying index (ID) of each stone type was obtained by calculating the integral under the drying curve.

Detailed discussion about the significance of these parameters is addressed below.

2.4 Statistical data analysis

To investigate the precision of the air permeability testing method the repeatability within specimen variation were evaluated. For this purpose, assuming that data distribution is unknown and that results are paired, a non-parametric hypothesis test for paired samples was used: the Wilcoxon test [23]. The test consists in calculating the algebraic differences for all pairs, ordering their absolute values in ascending order. Then sum the rank of the positive (or negative)
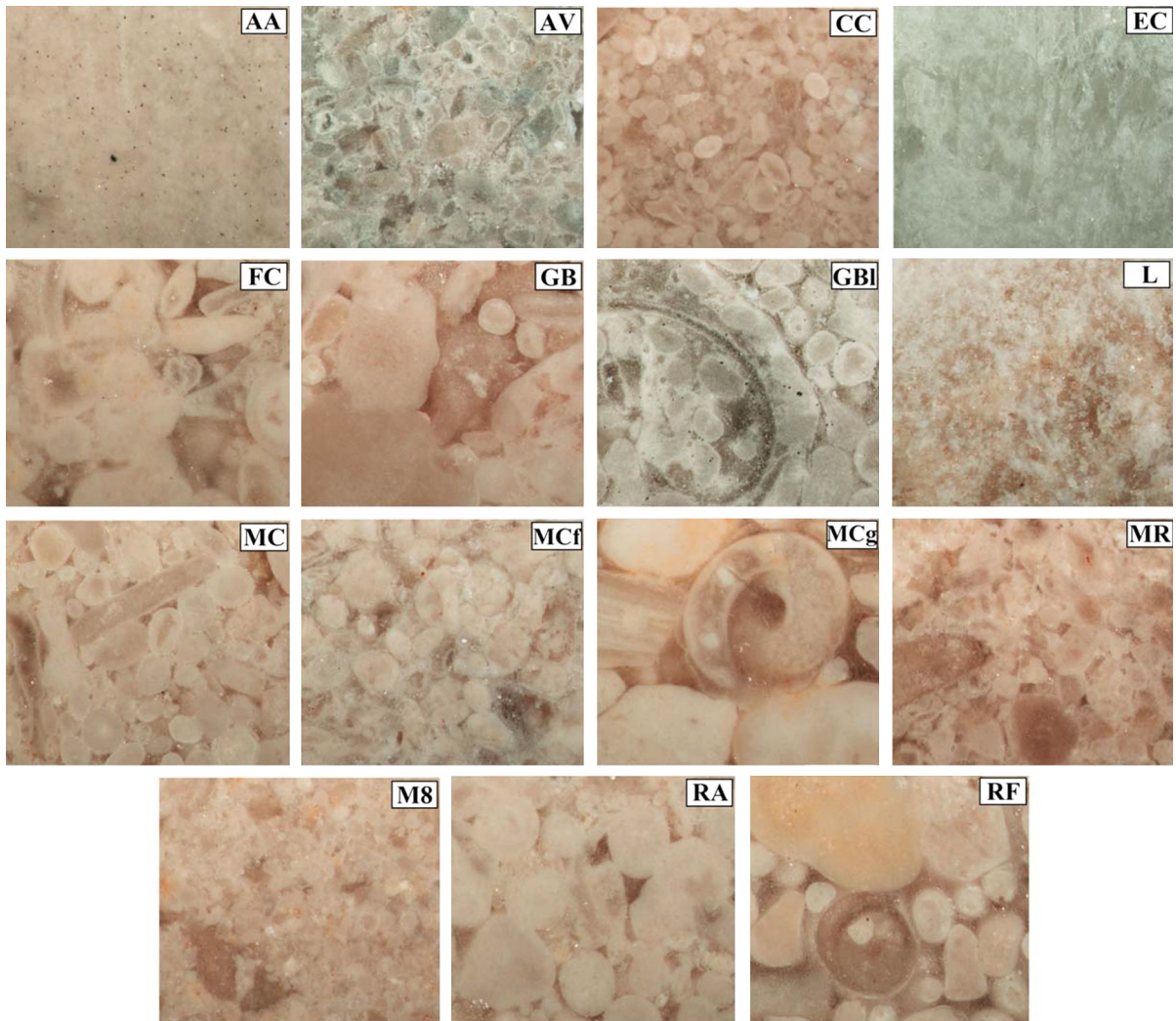
Fig. 1 Optical microphotographs of the different stones textures at same scale (field of view: 2.5 × 2.0 mm)

differences, being this value the test statistic. Finally, the test statistic is compared to a critical value from a reference table.

To verify if air permeability results are normally distributed, the Shapiro–Wilk hypothesis test [49] was used. The test statistic is:

$$W = \frac{\left(\sum_{i=1}^{n} a_i x_{(i)}\right)^2}{N \times s_N^2} \quad (2)$$

where W is the test statistic, N is the sample size, s_N is the uncorrected sample standard deviation, a_i are multiplying coefficients and $x_{(i)}$ is the ith smallest result in the sample.

The correlation analysis between kT values and the other parameters was performed using XLSTAT 2013 software and correlation coefficients (Pearson-r) were obtained. A statistic study was performed to assess if the correlation coefficients are statistically significant, according to the correlation test [59]:

$$t = r\sqrt{\frac{N-2}{1-r^2}} \quad (3)$$

where t is the statistic of correlation test, r is the correlation coefficient and N is the number of measurement pairs.

Table 2 Summary of stones grain sizes relations observed at binocular microscope

	<100 μm	100–200 μm	200–500 μm	500μ–1 mm	>1 mm
AA	++++	–	–	–	–
AV	+	++	+	–	–
CC	+	++	+	–	–
EC	++++	–	–	–	–
FC	–	+	+++	+++	–
GBl	–	++	++	++	++
GB	–	++	++	++	++
L	++++	–	–	–	–
MCf	+	+++	++	–	–
MCg	–	+	++	+++	+
MC	+	+++	+	–	–
M8	++++	+	+	–	+
MR	+	++	+++	–	–
RA	–	+	+++	++	–
RF	–	+	+	+++	+++

– none; + few; ++ some; +++ several; ++++ many

3 Results and discussion

3.1 Lithotypes characterization: grain size and geometry

In stones the grain geometry, size and its sorting have great importance in the porous network characteristics, especially in low consolidated stones. However, the textural features of consolidated stones are also influenced by other factors such as cementation and diagenetic processes. Figure 1 exhibits the textural features of the lithotypes described below, while Table 2 summarizes the relation of grain sizes in each stone variety, from observation at binocular stereoscope (magnifications up to 80×).

AA is a light-grey calciclastic limestone with bioclasts of very small grain impossible to distinguish at the used magnification.

AV is a grey calciclastic limestone, mainly oolitic of fine grain (<300 μm).

CC is a beige limestone, mainly composed by small oolites, generally with dimensions inferior to 200 μm.

EC is a white-beige crystalline marble with the rare presence of veins.

FC is a light beige limestone with thin to medium grain between 100 and 500 μm, essentially oolitic. Also, several pores were found through binocular stereoscope observation.

GBl is a grayish-blue limestone, coarsely calciclastic (sometimes, particles >4 mm) and bioclastic abundantly.

GB is a brownish-white limestone, coarsely calciclastic and bioclastic abundantly.

L is a microcrystalline carbonated stone of low temperature metamorphic facies [33]. The variety in study is a whitish-beige limestone conditioned by fossils debris.

Moca Creme has different beige varieties depending on the relation between grain and fossils sizes, representing different facies [14]. The MCg has the coarser texture, the grains are oolitic and bioclastic with intra-grain pores. The MCf has finer texture with smaller calciclastic particles, the oolites don't exceed 300 μm and the presence of bigger bioclasts is rare. At binocular stereoscope it was possible to identify several inter-grain voids corresponding to pores.

Moleanos limestones have several varieties depending on their texture. Generally, these stones are beige, calciclastic and composed by particles with different sizes. The MR is the most bioclastic with particles <1 mm, while M8 have bigger bioclasts (sometimes with 4 mm). The MC has small bioclasts but is predominantly oolitic (<250 μm).

RA is a white-cream calciclastic limestone, mainly oolitic, scarcely bioclastic. The majority of rounded particles are in the range of 200–500 μm. It were also identified several pores at binocular stereoscope.

RF is a cream-beige limestone, oolitic and bioclastic. The oolitic particles have dimensions between 100 μm and 2 mm, while the bioclasts are generally smaller than 3 mm.

Table 3 Values of some transport-related properties of the stones obtained by using standardized tests

	P_o (%)	ρ_b (kg/m^3)	A_b (%)	AC g/(m^2 s$^{1/2}$)	ID	$A_{bv}-A_b$ (%)
AA	1.19 ± 0.01	2,674.1 ± 0.0(3)	0.45 ± 0.02	0.36 ± 0.02	0.160 ± 0.014	0.01
AV	2.18 ± 0.04	2,637.9 ± 2.2	0.83 ± 0.02	0.66 ± 0.01	0.170 ± 0.003	0.00
CC	10.15 ± 0.38	2,396.4 ± 7.7	4.64 ± 0.04	31.02 ± 0.81	0.180 ± 0.007	0.40
EC	0.24 ± 0.03	2,708.4 ± 0.8	0.09 ± 0.00(4)	0.31 ± 0.02	0.055 ± 0.005	0.00
FC	15.38 ± 0.26	2,250.66 ± 6.5	7.24 ± 0.12	67.33 ± 1.20	0.227 ± 0.032	0.40
GBl	2.70 ± 0.07	2,623.3 ± 2.4	1.10 ± 0.03	3.12 ± 0.03	0.153 ± 0.002	0.07
GB	3.65 ± 0.31	2,595.9 ± 8.9	1.48 ± 0.26	3.11 ± 0.32	0.119 ± 0.008	0.07
L	0.56 ± 0.10	2,692.3 ± 3.2	0.21 ± 0.04	0.18 ± 0.03	0.148 ± 0.020	0.00
MCf	12.99 ± 0.04	2,299.7 ± 0.7	6.00 ± 0.05	42.56 ± 1.15	0.170 ± 0.005	0.35
MCg	9.52 ± 0.22	2,419.0 ± 9.1	4.18 ± 0.39	25.48 ± 4.33	0.165 ± 0.012	0.24
MC	6.54 ± 0.13	2,505.7 ± 4.2	2.79 ± 0.05	16.80 ± 2.33	0.115 ± 0.007	0.18
M8	8.57 ± 0.55	2,441.9 ± 12.9	3.70 ± 0.01	19.66 ± 0.62	0.133 ± 0.008	0.19
MR	9.21 ± 0.23	2,427.4 ± 5.5	3.93 ± 0.26	24.56 ± 2.60	0.152 ± 0.011	0.14
RA	17.19 ± 0.01	2,211.47 ± 0.0(4)	7.75 ± 0.30	81.62 ± 3.85	0.276 ± 0.030	−0.03
RF	6.45 ± 0.22	2,480.9 ± 3.4	3.37 ± 0.22	11.42 ± 0.83	0.139 ± 0.009	0.77

3.2 Porosity, density and hydric properties

Table 3 shows the calculated values of open porosity (P_o), apparent density (ρ_b), water absorption (A_b), capillary water absorption coefficient (AC) and drying index (ID). The presented values are the mean values of the stones samples used in this work and do not necessarily represent the mean characteristics of each lithotype. For commercial purposes, the certificate of mean characteristics from technical sheets of each stone must be consulted.

As expected, significant differences were found in the porosity values determined for the fifteen lithotypes, ranging from 0.24 to 17.19 %. EC has the lowest porosity followed by L (0.56 %). This data is in accordance with previous description since these stones suffered different metamorphization degrees; the crystallization processes reduced the volume of pores.

On the other hand, RA and FC have the higher porosity values, which is in agreement with the observation through binocular stereoscope.

The apparent density values obtained are between 2,212 and 2,708 kg/m^3. This parameter calculation is deeply associated with open porosity [17] and consequently the density sequence of the stones from the highest to lowest, is inversely proportional to the open porosity sequence.

Concerning water absorption at atmospheric pressure, the trend is equal to the trend of open porosity values. It is obvious that the water fills the accessible pores and thus increased open porosity produce higher water absorption (by total immersion). However, since the tests were performed under different conditions, at vacuum and atmospheric pressure, to extract more qualitative information about the porous media an exercise can be made: comparing the percentage of water absorption induced by the vacuum (A_{bv}) and the one obtained at atmospheric pressure (A_b) (Table 3, last column). This analysis enabled to observe that for low water absorption (<2 %) the values obtained by the two methods are the same, but in lithotypes with higher water absorptions the values of water absorption under vacuum conditions have tendency to increase in relation to those obtain under atmospheric pressure (except RA). Similar behavior was also verified elsewhere [52]. The lower values obtained at atmospheric pressure could be explained by the air trapped inside the pores and since the exchanges air/solution occurs along the same path [6], the ultimate exchanges occur only under vacuum conditions (in a reasonable period of time). It has been shown that really full saturation with nearly constant values can be achieved only at tests with durations up to 2 years [51]. These differences could give indirect information about the tortuosity/complexity of the porous
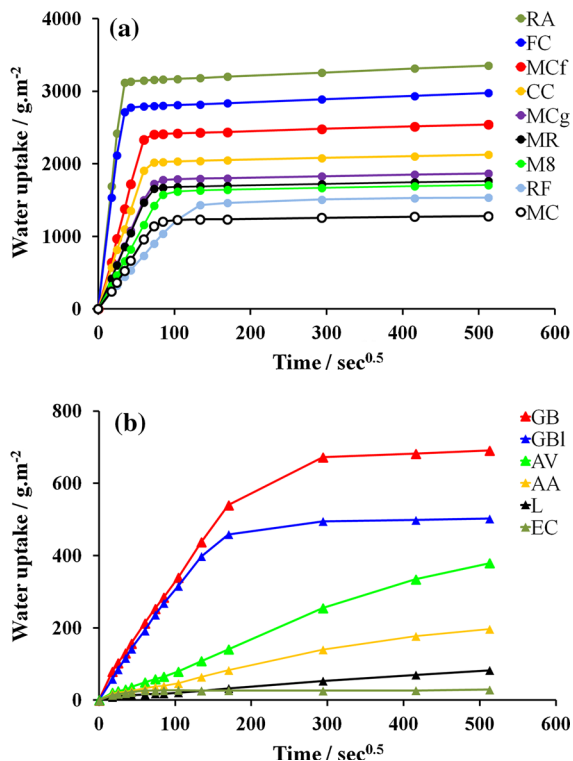
Fig. 2 Capillary suction curves of stones varieties: **a** high porous stones, **b** low porous stones

system. Higher differences are a result of a more tortuous and unconnected media.

If the previous determinations provide direct information about the total volume of voids, the capillary water absorption coefficient gives other useful indications about the pore system [24, 48]. The capillary absorption forces are originated in pores with diameters between 1 μm and 1 mm, whereas the larger capillaries have higher suction velocities and lower suction power and smaller capillaries have lower suction velocities and higher suction power [51].

From the curves of capillary penetration (Fig. 2), the slope of the first linear part was considered to calculate the capillary coefficient. Therefore, the capillary coefficient value is influenced by the majority of the pore system parameters.

The lithotypes revealed a wide range of values of capillary water absorption coefficients, from 0.18 g m^{-2} s$^{-1/2}$ (L) to 81.62 g m^{-2} s$^{-1/2}$ (RA). This emphasizes the differences between pore systems and thus the transport kinetics behavior of stones.

Except in the case of stones with very low porosity (L and EC), a similar trend between the open porosity and capillary coefficient can be observed, the higher the open porosity, the higher the capillary coefficient values. However, this relation is non-linear, i.e., the ratio AC/P_o tends to increase with higher porosities.

Complementing the water absorption and capillary water absorption coefficient are the drying mechanisms related to the movement of the fluid water and vapor out of the pore system [51]. The drying process is generally characterized by two distinct phases: (i) in the first stage the water loss is high and constant along time as consequence of the capillary water movement from the inside to the surface, which remains wet if the water moves quickly enough to compensate the evaporation rate. This stage is essentially managed by the surrounding conditions, i.e., by the potential evaporation of the environment [18, 19]. (ii) in the second stage the continuous transport of water to the surface is no longer possible and only the water vapor processes remain at a low and constant rate.

The transition from the first to the second phase is usually characterized by a non-constant and small water loss. The time of transition between this two drying phases is called knick-point. The drying process stops when the moisture content of samples and the surrounding environment are in equilibrium [15]. Figure 3 shows the mean drying curves obtained for the lithotypes. Not all the stones revealed a drying behavior in accordance to the description previously made. In some stones, the first phase of drying shows a two step flux, quite evident for the RA samples. Within the first phase, the drying starts at relatively low rate and then is followed by a maximum drying rate. Although similar behaviors having been reported in literature, this phenomenon is difficult to explain. The two flux rates in first stage were attributed to characteristic specific inner surfaces in terms of surface roughness that influences the evaporation initial rate [15, 58]. Such explanation is quite reasonable since the experimental data revealed a predominance of this phenomenon in more porous stones. On the other hand, in lithotypes with very low porosity (e.g. EC case), the transition between the two drying phases is not clear and occurs at very early stages. Phase I is fast and hardly perceptible by gravimetric measurements owing to small water content in low porous stones (even when saturated), and to the
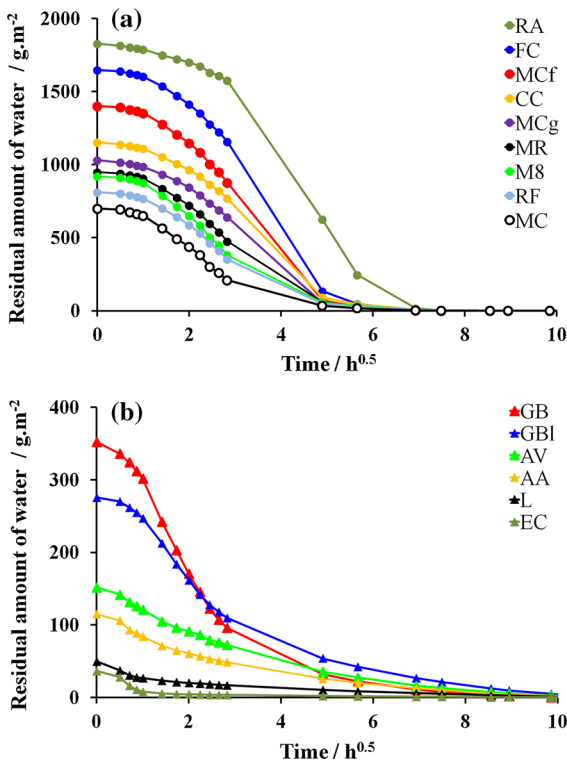
Fig. 3 Drying curves of stones with different behaviors: **a** high porous stones, **b** low porous stones

Fig. 4 Relation between measurements at the same position (kT_1-measurement one; kT_2-measuremente two)

specific potential evaporation which controls the first stage of evaporation.

Due to different behaviors between low and high porous stones, the D_I and D_{II} were not calculated; instead, the drying index of each stone is given in Table 3. This index is appropriate to compare drying behaviors [11]. The registered values of ID are in accordance with the other stones properties, i.e., the amount of evaporated water is superior in more porous stones. Furthermore, these stones need shorter times to achieve constant mass, a trend that indicates good connection between pores.

Stones with smaller grain size have lower porosities and slower water transport kinetics; the results also suggest that the grain boundaries, which are mainly governed by cementation and diagenetic crystallization processes, have a more important role. This statement has also been reported by other authors [51].

3.3 Air-permeability

The measurements performed on four stones, L, EC, EV and AA revealed values inferior to 0.001×10^{-16} m^2,

which are below the minimum reading limit value. Even so, the equipment provides the values of the pressure rise in the inner chamber at the end of the test (ΔP_i), after 720 s, showing some sensibility to permeabilities below this limit. In these cases, the higher value was obtained in EC and the lower in AV, indicating that EC has higher and AV the lower permeability. This relation is not consistent with the parameters obtained from the above mentioned standardized tests. Therefore, under this limit of 0.001×10^{-16} m^2, the measurements from Torrent permeability test are considered as not reliable. Thus, it is possible to claim that this method is not applicable to dimensions stones with water absorption values equal or inferior to 0.8 % and open porosities ≤2.2 % (AV). Due to this reason, further analysis will involve only the stone varieties with values above these limits.

On the remaining stone varieties, a wide range of kT values were obtained, between 0.0022×10^{-16} m^2 (GBl) and 7.5×10^{-16} m^2 (RA), which emphasizes the different pore-network characteristics. For similar lithotypes, the range of values is in good agreement with the only reference concerning measuring kT on stones [4].

Figure 4 shows the relation between measurements made on the same stone and on the same position. For all the tested range (0.0022×10^{-16} to 7.5×10^{-16} m^2) the differences between two measurements seem irrelevant. The Wilcoxon test (2.4) indicated a null difference between first and second sets of measurements (p value = 0.432).
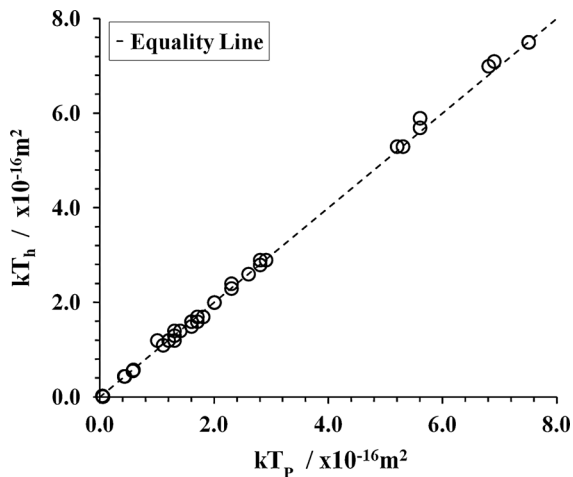
Fig. 5 Relation between measurements at surfaces with different finishing (kT_p—polished; kT_h—honed)

Fig. 6 Relation between measurements at different samples (same stone)

In fairly dry stones with permeability values within the tested range, the Torrent permeability test method provides accurate and repeatable measurements.

Comparing measurements made on surfaces with different finishes (polished and honed), presented in Fig. 5, it was possible to observe also irrelevant differences between measurements on both surface types. The Wilcoxon test (2.4), applied to the first sets of measurements, indicated a null difference between kT in polished and honed surfaces (p value = 0.302). It is believed that these types of surface have different specific surface areas and interestingly, it seems that these variations do not affect the instrument readings. Although not tested, in surfaces with rougher finishes, such as bush-hammered, due to difficulties in the isolation of the two separate chambers, the application of the method could become difficult.

The relation between results of the measurements made on the same variety but on different samples is depicted in Fig. 6. In this case, there is some data spread from the equality line. This exhibits some heterogeneity, typical of natural materials; this characteristic is what makes so attractive the natural dimension stones as an ornamental material for buildings. Nevertheless, the Wilcoxon test (2.4), applied to the first sets of measurements, indicated a null difference between kT in both specimens of the same stone (p value = 0.383).

The hypothesis that the kT results follow a normal distribution was tested using the Shapiro–Wilk test
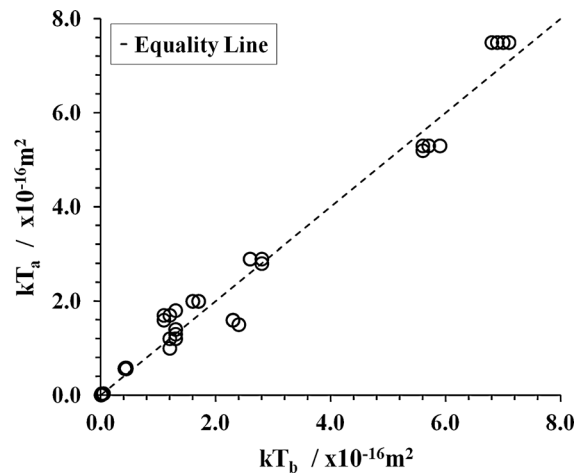
Table 4 Shapiro–Wilk test results for kT samples

Sample	Test statistic (W)	p value
CC	0.752	0.009
FC	0.895	0.262
GB	0.866	0.282
GBl	0.940	0.615
M8	0.794	0.025
MC	0.756	0.009
MCf	0.757	0.010
MCg	0.641	≈ 0
MR	0.861	0.122
RA	0.799	0.028
RF	0.760	0.011

(2.4) at a significance level of 5 %. Since there were no kT differences between measurements in specimens or surfaces, each stone is represented by a set of eight results. The tested hypothesis was rejected in seven of the eleven sets, as shown in Table 4. There is a substantial part of the results that does not fit a Normal distribution. Actually, Neves et al. [37] found similar results when applying the Torrent method on concrete samples. In such cases, they propose the use of the median of air permeability results as a central value. Table 5 presents the median and interquartile range values of kT obtained from eight measurements on each stone variety.

Table 5 Median and interquartile range of kT values obtained from the eight measurements made in slabs (polish and honed surfaces)

Sample	kT ($\times 10^{-16}$ m^2)
AA	<0.001(ΔP_i = 2.90 mbar—720 s)
AV	<0.001(ΔP_i = 2.50 mbar—720 s)
CC	1.850; 0.375
EC	<0.001 (ΔP_i = 3.60 mbar—720 s)
FC	5.450; 0.375
GB	0.033; 0.020
GBl	0.003; 0.003
L	<0.001 (ΔP_i = 3.10 mbar—720 s)
M8	1.300; 0.100
MC	1.200; 0.075
MCf	2.800; 0.250
MCg	1.950; 0.700
MR	1.450; 0.575
RA	7.300; 0.575
RF	0.503; 0.145

3.4 Relationships between air-permeability and other transport-related properties

Since a very small dispersion was obtained in the previous determinations, only the median values of kT and mean values of the other properties will be considered for further analysis in this section.

The relationship between the permeability and porosity of several materials has been in study for several decades. Depending on the materials, various approaches more or less complex could be found in literature. This type of relation, between permeability and porosity, is usually performed in geosciences to predict the permeability of rocks formations, which is key parameter to assess their capabilities as geological reservoirs (water, geothermal, oil and gas, etc.) [35, 62]. Therefore, different types of models have been proposed [35]. According to the experimental data, this physical relation could be described in mathematical terms by an exponential law [20, 28]:

$$k = a_1 \emptyset^{b_1} \tag{4}$$

where k is permeability, $\emptyset$ is porosity, a_1 and b_1 are constants.

Figure 7 shows graphically the correlation between the two sets of mean values of open porosity and median values of air-permeability of the stones. In other materials such as concrete, representing the
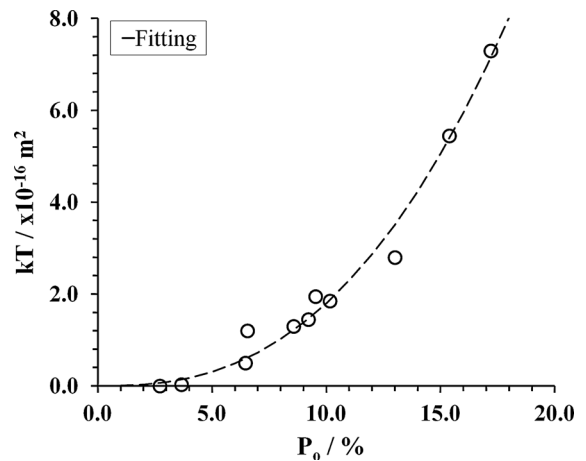
Fig. 7 Experimental correlation between air-permeability (kT) and open porosity (P_o)
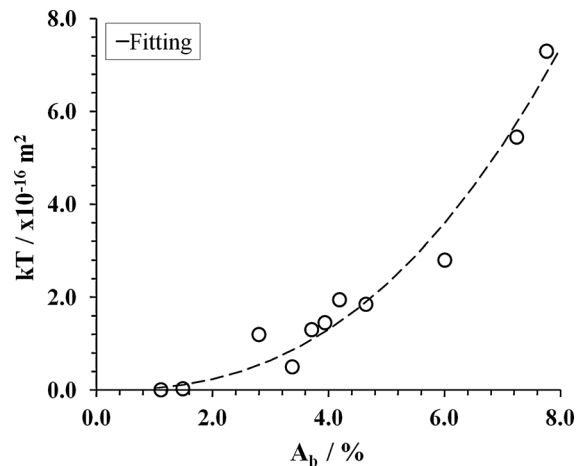
Fig. 8 Experimental correlation between air-permeability (kT) and water absorption (A_b)

permeability as a function of porosity alone could be not adequate [34]. However, this experimental correlation reveals a structured non-linear relation between the two parameters. The exponential law represented in (4), was graphically fitted to the experimental data with good correlation ($r = 0.98$, $t_{(9)} = 15.7$, $p < 0.05$). Even though the number of samples is small for a universal relation, it was possible to formulate an analytic relation for the stones and range of values under study:

$$kT\left(\times 10^{-16} \text{m}^2\right) = 5.17 \times 10^{-3} \times P_0^{2.54}(\%) \tag{5}$$
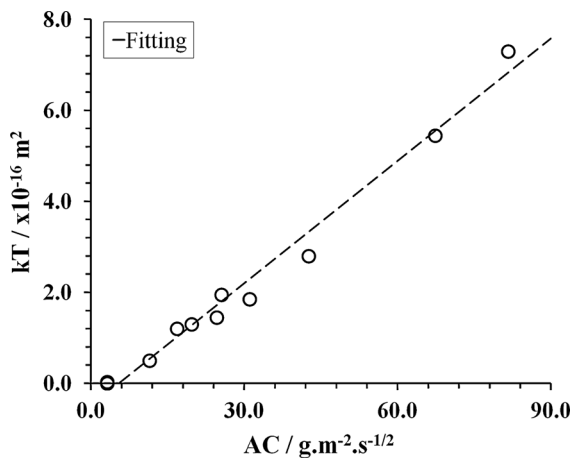
Fig. 9 Experimental correlation between air-permeability (*kT*) and capillary water absorption coefficient (AC)

A similar relation was found between *kT* and A_b (Fig. 8) and Eq. 6 was obtained.

$$kT\left(\times 10^{-16} \text{m}^2\right) = 4.11 \times 10^{-2} \times A_b^{2.49}(\%) \qquad (6)$$

It is a fact that open porosity or water absorption only characterizes the volume of voids inside the material, while the permeability takes into account other features such as tortuosity and pore sizes.

Figure 9 presents the relation between *kT* and AC values. The representation highlights the interconnection between these two parameters ($r = 0.99$, $t_{(9)} = 22.2$, $p < 0.05$) and contrary to what was found in the previous cases, this type of correlation has a linear trend (Eq. 7). AC has the contribution of more characteristics of the pore structure and not only the volume of voids, in particular tortuosity and pore sizes. This parameter is a geometric characteristic of a porous material and takes into account the pore thickness, geometry and its trajectory [39]. Several equations to determine the tortuosity value of porous materials have been discussed [5, 39]. Despite the tortuosity being indeed an important parameter in the characterization of a porous medium, a deeper analysis is outside the purpose of this paper and therefore will be left for further works.

Nevertheless, knowing the *kT* value it is possible to estimate with good accuracy the capillary absorption coefficient of a carbonated stone.

$$kT\left(\times 10^{-16} \text{m}^2\right) = 0.0897 \times \text{AC}\left(\text{g m}^{-2}\text{ s}^{-1/2}\right) \\ - 0.496 \qquad (7)$$
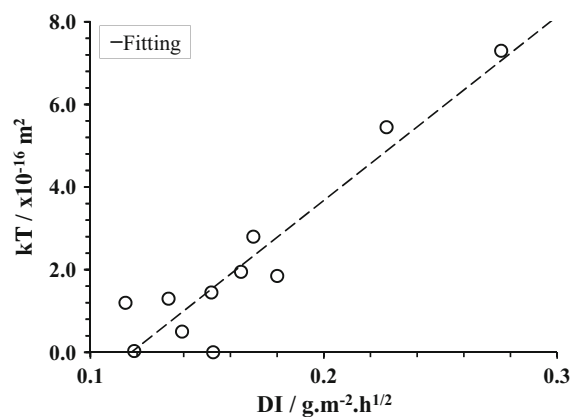

Fig. 10 Experimental correlation between air-permeability (*kT*) and drying index (ID)

$$kT\left(\times 10^{-16}\text{m}^2\right) = 44.55 \times \text{ID}\left(\text{g m}^{-2}\text{ h}^{1/2}\right) - 5.24 \qquad (8)$$

Figure 10 exhibits the experimental correlation between air-permeability (*kT*) and drying index. Despite some dispersion, the correlation coefficient is statistically significant ($r = 0.94$, $t_{(9)} = 8.12$, $p < 0.05$) and, therefore, a significant relationship between air-permeability (*kT*) and drying index it was also found (Eq. 8).

kT value gives a good quantification of the internal structure and reflects its differences. It is believed that the method can also contribute in monitoring alterations due to weathering processes, i.e., to evaluate the degradation degree of a stone in use or to quantify changes in the internal structure after laboratorial accelerated aging tests.

As previously mentioned, the physical characteristics give important indications about the weathering resistance of stones. Various graded classifications were established according to physical values with the purpose of providing information for a proper application of stones in buildings. Stones could be graded, based on water absorption and open porosity values, according to Table 6 [41] and it is possible to use Eqs. 4 and 5 to establish similar classes for *kT* values. The stones in class I_a ($A_b < 0.5$ %) with *kT* values inferior to 0.008×10^{-16} m^2 are appropriate for exterior uses in moist environments, while stones with *kT* value above 12.7×10^{-16} m^2 (class III) should be used in interior zones with no exposure to aggressive agents.

Table 6 Classification of stones for construction purposes according to water absorption and open porosity values

A_b Class	I_a	I_b	II_a	II_b	III
A_b (%)	0–0.5	0.5–3	3–6	6–10	>10
kT ($\times 10^{-16}$ m^2)	0.000–0.009	0.009–0.842	0.842–4.898	4.898–17.926	>17.926

P_o Class	Very low	Low	Low/Medium	Medium	High	Very high
P_o (%)	0–0.5	0.5–1	1–3	3–6	6–10	>10
kT ($\times 10^{-16}$ m^2)	0–0.007	0.007–0.041	0.041–0.633	0.633–3.560	3.560–12.701	>12.701

Concerning capillary suction coefficient, analogous approach can be performed; for values <60 g m^{-} s$^{-1/2}$ the stone is considered suitable for application on exterior exposed zones and for values between 60 and 160 g m^{-2} s$^{-1/2}$ the stone is appropriate for exterior uses in non-exposed zones [41]. In terms of kT values, the respective limits are 4.9×10^{-16} and 13.8×10^{-16} m^2.

The determination of the maximum limit for kT was slightly inaccurate (12.7 to 13.8×10^{-16} m^2) as a result of absence of lithotypes in that range of values.

4 Conclusions

The studied stones reveal a wide range of physical characteristics. The "Torrent" permeability test proved to be a suitable method to measure the air-permeability, performing accurate and reproducible measurements on dimension stones with open porosity above 2 %. It is a non-destructive method that can be used in laboratory and on site and can be applied as complementary or as an alternative method to the traditional ones.

The fluid transport kinetics of the studied stones are mainly governed by textural features, cementation, diagenetic and crystallization processes.

There is an exponential relation between air-permeability and open porosity or water absorption. For the capillary suction coefficient a linear trend was found. It is believed that significant moisture content can affect kT absolute values, and therefore these close relationships are valid under the test conditions reported, i.e., fairly dry stones.

The air-permeability can provide indications about the stone susceptibility to decay. The stones with kT values <0.008×10^{-16} m^2 are appropriate for exterior uses in moist environments, while stones with value above 12.7×10^{-16} m^2 should be used in interior zones with no exposure to aggressive agents.

References

1. Andriani G, Walsh N (2003) Fabric, porosity and water permeability of calcarenites from Apulia (SE Italy) used as building and ornamental stone. Bull Eng Geol Environ 62(1):77–84. doi:10.1007/s10064-002-0174-1
2. Angeli M, Benavente D, Bigas J-P, Menéndez B, Hébert R, David C (2008) Modification of the porous network by salt crystallization in experimentally weathered sedimentary stones. Mater Struct 41(6):1091–1108. doi:10.1617/s11527-007-9308-z
3. Barros RS, Oliveira DV, Varum H, Alves CAS, Camões A (2014) Experimental characterization of physical and mechanical properties of schist from Portugal. Constr Build Mater 50:617–630. doi:10.1016/j.conbuildmat.2013.10.008
4. Bueno V (2004) Estudio de Factibilidad de un Nuevo Ensayo de Permeabilidad en Rocas. Univ. del Zulia, Maracaibo, p 88
5. Cai J, Yu B (2011) A discussion of the effect of tortuosity on the capillary imbibition in porous media. Transp Porous Media 89(2):251–263. doi:10.1007/s11242-011-9767-0
6. Castela AS, Sena da Fonseca B, Duarte RG, Neves R, Montemor MF (2014) Influence of unsupported concrete media in corrosion assessment for steel reinforcing concrete by electrochemical impedance spectroscopy. Electrochim Acta 124:52–60. doi:10.1016/j.electacta.2013.11.157
7. CEN (2000) Natural stone test methods: determination of water absorption coefficient by capillary. EN 1925
8. CEN (2001) Natural stone test methods: determination of real density and apparent density, and of total and open porosity. EN 1936
9. CEN (2005) Natural stone test methods: determination of water absorption at atmospheric pressure. EN 13755
10. CEN (2010) Conservation of cultural property: determination of water vapour permeability. EN 15803
11. CEN (2013) Conservation of cultural property: determination of drying properties. EN 16322

12. Commission 25-PEM R (2006) Water absorption tube test. Test method II.4

13. Denariè E, Jacobs F, Leeman A, Teruzzi T, Torrent R (2011) Specification and site control of the permeability of the cover concrete: the Swiss approach. Paper presented at the international RILEM conference on advances in construction materials through science and engineering, pp 478–485

14. Figueiredo C, Folha R, Maurício A, Alves C, Aires-Barros L (2010) Pore structure and durability of Portuguese limestones: a case study. Limestone in the building environment: present day challenges for the preservation of the past, vol 331. Geological Society, London, pp 157–169

15. Franzen C, Mirwald PW (2004) Moisture content of natural stone: static and dynamic equilibrium with atmospheric humidity. Environ Geol 46(3–4):391–401. doi:10.1007/s00254-004-1040-1

16. García O, Malaga K (2012) Definition of the procedure to determine the suitability and durability of an anti-graffiti product for application on cultural heritage porous materials. J Cult Herit 13(1):77–82. doi:10.1016/j.culher.2011.07.004

17. Hall C, Hamilton A (2013) Porosity–density relations in stone and brick materials. Mater Struct 1–7. doi:10.1617/s11527-013-0231-1

18. Hall C, Hoff W (2002) Water transport in brick, stone, and concrete. Taylor & Francis, Oxon, p 318

19. Hall C, Hoff WD, Nixon MR (1984) Water movement in porous building materials—VI. Evaporation and drying in brick and block materials. Build Environ 19(1):13–20. doi:10.1016/0360-1323(84)90009-X

20. Heigold PC, Gilkeson RH, Castwright K, Reed PC (1980) Aquifer transmissivity from surficial electrical measurements. Groundwater 17:330–345

21. Hendrickx R (2013) Using the Karsten tube to estimate water transport parameters of porous building materials. Mater Struct 46(8):1309–1320. doi:10.1617/s11527-012-9975-2

22. Hoigard KR (2000) Dimension stone cladding: design, construction, evaluation, and repair, vol 1394. ASTM, West Conshohocken, p 184

23. Hollander M, Wolfe D (1999) Nonparametric statistical methods. Wiley, New York, p 816

24. Karaca Z (2010) Water absorption and dehydration of natural stones versus time. Constr Build Mater 24(5):786–790. doi:10.1016/j.conbuildmat.2009.10.029

25. Kourkoulis SK, Ganniari-Papageorgiou E (2010) Experimental study of the size- and shape-effects of natural building stones. Constr Build Mater 24(5):803–810. doi:10.1016/j.conbuildmat.2009.10.027

26. Kucharczyková B, Misák P, Vymazal T (2010) The Air-permeability measurement by torrent permeability tester. In: Proceedings of the 10th international conference on modern building materials, structures and techniques, Vilnius, 2010, pp 162–166

27. La Russa MF, Ruffolo SA, Rovella N, Belfiore CM, Palermo AM, Guzzi MT, Crisci GM (2012) Multifunctional TiO$_2$ coatings for cultural heritage. Prog Org Coat 74(1):186–191. doi:10.1016/j.porgcoat.2011.12.008

28. Lima OAL, Niwas S (2000) Estimation of hydraulic parameters of shaly sandstone aquifers from geoelectrical measurements. J Hydrol 235(1–2):12–26. doi:10.1016/S0022-1694(00)00256-0

29. Lombillo I, Thomas C, Villegas L, Fernández-Álvarez JP, Norambuena-Contreras J (2013) Mechanical characterization of rubble stone masonry walls using non and minor destructive tests. Constr Build Mater 43:266–277. doi:10.1016/j.conbuildmat.2013.02.007

30. Lopez-Arce P, Doehne E, Greenshields J, Benavente D, Young D (2009) Treatment of rising damp and salt decay: the historic masonry buildings of Adelaide, South Australia. Mater Struct 42(6):827–848. doi:10.1617/s11527-008-9427-1

31. Martinho E, Dionísio A, Almeida F, Mendes M, Grangeia C (2014) Integrated geophysical approach for stone decay diagnosis in cultural heritage. Constr Build Mater 52:345–352. doi:10.1016/j.conbuildmat.2013.11.047

32. MAS (2013) [www.m-a-s.com.ar/]. Accessed April 2013

33. Miller AZ, Leal N, Liaz L, Regerio-Candelera MA, Silva RJC, Dionísio A, Macedo MF, Saiz-Jimenez C (2010) Primary bioreceptivity of limestones used in Southern European monuments. Limestone in the building environment: present day challenges for the preservation of the past, vol 331. Geological Society, London, pp 79–92

34. Neithalath N, Sumanasooriya MS, Deo O (2010) Characterizing pore volume, sizes, and connectivity in pervious concretes for permeability prediction. Mater Charact 61(8):802–813. doi:10.1016/j.matchar.2010.05.004

35. Nelson P (1994) Permeability–porosity relationships in sedimentary rocks. Log Analyst 35:38–62

36. Neves R (2012) A permeabilidade ao ar e a carbonatação do betão nas estruturas. ULisboa—IST, Lisboa, p 416

37. Neves R, Branco F, Brito J (2012) About the statistical interpretation of air permeability assessment results. Mater Struct 45(4):529–539. doi:10.1617/s11527-011-9780-3

38. Nicholson DT (2001) Pore properties as indicators of breakdown mechanisms in experimentally weathered limestones. Earth Surf Proc Landf 26(8):819–838. doi:10.1002/esp.228

39. Nikitsin VI, Backiel-Brzozowska B (2013) Determination of capillary tortuosity coefficient in calculations of moisture transfer in building materials. Int J Heat Mass Transf 56(1–2):30–34. doi:10.1016/j.ijheatmasstransfer.2012.09.021

40. Pinna D, Salvadori B, Porcinai S (2011) Evaluation of the application conditions of artificial protection treatments on salt-laden limestones and marble. Constr Build Mater 25(5):2723–2732. doi:10.1016/j.conbuildmat.2010.12.023

41. Pinto A, Alho A, Moura A, Henriques A, Carvalho C, Ramos J, Almeira N, Mestre V (2006) Manual da pedra natural para arquitectura. Direcção-Geral de Geologia e Energia, p 194

42. Přikryl R, Smith BJ (2007) Building stone decay: from diagnosis to conservation. Geological Society of London, London, p 330

43. Quagliarini E, Bondioli F, Goffredo GB, Cordoni C, Munafò P (2012) Self-cleaning and de-polluting stone surfaces: TiO$_2$ nanoparticles for limestone. Constr Build Mater 37:51–57. doi:10.1016/j.conbuildmat.2012.07.006

44. Quagliarini E, Bondioli F, Goffredo GB, Licciulli A, Munafò P (2013) Self-cleaning materials on architectural heritage: compatibility of photo-induced hydrophilicity of

TiO$_2$ coatings on stone surfaces. J Cult Herit 14(1):1–7. doi:10.1016/j.culher.2012.02.006

45. Reyes J, Corvo F, Espinosa-Morales Y, Dzul B, Perez T, Valdes C, Aguilar D, Quintana P (2011) Influence of air pollution on degradation of historic buildings at the urban tropical atmosphere of San Francisco de Campeche City, México. In: Monitoring, control and effects of air pollution. InTech, pp 201–226

46. Romer M (2005) Effect of moisture and concrete composition on the torrent permeability measurement. Mater Struct 38(5):541–547. doi:10.1007/bf02479545

47. Sarıışık G, Sarıışık A, Gökay MK (2013) Investigation the glazability of dimension andesites with glaze coating materials containing boron minerals in construction sector. Mater Struct 46(9):1507–1517. doi:10.1617/s11527-012-9992-1

48. Sena da Fonseca B, Vilão A, Galhano C, Simão JAR (2014) Reusing coffee waste in manufacture of ceramics for construction. Adv Appl Ceram 113(3):159–166. doi:10.1179/1743676113y.0000000131

49. Shapiro S, Wilk M (1965) An analysis of variance test for normality (complete samples). Biometrika 52(3-4):591–611

50. SIA (2003) Construction en béton—Spécifications complémentaires, Annexe E: Perméabilité à l'air dans les Structures. SIA 262/1

51. Siegesmund S, Dürrast H (2011) Physical and mechanical properties of rocks. Stone in architecture, 4th edn. Springer, Berlin, pp 97–225

52. Siegesmund S, Grimm W, Durrast H, Ruedrich J (2010) Limestones in Germany used as building stones: an overview. Limestone in the building environment: present day challenges for the preservation of the past. Geological Society, London, pp 37–59

53. Siegesmund S, Török Á (2011) Building stones. In: Siegesmund S, Snethlage R (eds) Stone in architecture. Springer, Berlin, Heidelberg, pp 11–95. doi:10.1007/978-3-642-14475-2_2

54. Silva ZSG, Simão JAR (2009) The role of salt fog on alteration of dimension stone. Constr Build Mater 23(11):3321–3327. doi:10.1016/j.conbuildmat.2009.06.044

55. Torrent R (1992) A two-chamber vacuum cell for measuring the coefficient of permeability to air of the concrete cover on site. Mater Struct 25(6):358–365. doi:10.1007/bf02472595

56. Torrent R (2013) Non-destructive site air-permeability test—relation with other transport test methods. Materials Advanced Services Ltd, Buenos Aires, www.m-a-s.com.ar. Nov 2013

57. Torrent R, Basheer M, Gonçalves AF (2007) Non-destructive methods to measure gas-permeability (Chapter 3). TC 189-NEC: State-of-the-Art Report. RILEM, 35–66

58. Tournier B, Jeannette D, Destrigneville C (2000) Stone drying: an approach of the effective evaporating surface area In: Proceedings of 9th international congress on deterioration and conservation of stone, Venice, 2000, pp 629–635

59. Urdan T (2005) Statistics in plain english—second edition. Lawrence Erlbaum Associates, Mahwah, p 184

60. Vandevoorde D, Cnudde V, Dewanckele J, Brabant L, de Bouw M, Meynen V, Verhaeven E (2013) Validation of in situ applicable measuring techniques for analysis of the water adsorption by stone. Procedia Chem 8:317–327. doi:10.1016/j.proche.2013.03.039

61. Vázquez P, Alonso FJ, Carrizo L, Molina E, Cultrone G, Blanco M, Zamora I (2013) Evaluation of the petrophysical properties of sedimentary building stones in order to establish quality criteria. Constr Build Mater 41:868–878. doi:10.1016/j.conbuildmat.2012.12.026

62. Weibel R, Kristensen L, Olivarius M, Hjuler ML, Mathiesen A, Nielsen LH (2012) Investigating deviations from overall porosity-permeability trends. Paper presented at the proceedings 36th workshop on geothermal reservoir engineering, Stanford University, California, p 16